TIME-DOMAIN CALIBRATION METHOD FOR CHANNEL RESPONSE OF BROADBAND RECEIVING ARRAY ANTENNA

Hao Zeng[1,2], Jianwen Zhou[1], Qingkun Yang[1] and Haidan He[2]

[1]Electronic Engineering Department
Chongqing University
No. 174, Shazheng Street, Shapingba District, Chongqing 400044, P. R. China

[2]Southwest China Institute of Electronic Technology
No. 85, West Yingkang Road, Jinniu District, Chengdu 610036, P. R. China
haoz@cqu.edu.cn

ABSTRACT. *Channel amplitude and phase errors of broadband receiving array antenna will affect the performance of the array system deeply. So it is required to be calibrated before digital beamforming. The chirp signal as reference signal cannot achieve a stable weight vector, because it is non-stationary. According to channel equalization principle, a time-domain calibration method is presented where the broadband Binary Phase Shift Keying (BPSK) signal is employed as the reference signal. The iterative algorithm is introduced firstly. Then, the effects of various parameters to calibration accuracy are analyzed. Simulation results illustrate that new time-domain calibration methodology overcomes the mismatch of wideband receiver array antenna correctly.*
Keywords: Array antenna, Time domain filtering, Channel calibration, LMS algorithm

1. **Introduction.** Array antenna system is widely used in military and civilian industries because of its excellent anti-jam function [1]. In broadband receiving array antenna system [2,3], RF front-end is composed of low noise amplifier, mixer, filter, IF amplifier and other analog devices. As described in [4,5], various reasons will make the channel responses in amplitude and phase different from each other. Therefore, the channel errors must be calibrated.

Current broadband calibration methods could be classified into frequency-domain and time-domain methods. Frequency-domain calibration in [6,7] converts the broadband signal into a serial of narrow band signals. So the calibration algorithm for narrow band array could be used easily. However, these processes are very complex since Fourier transform and inverse Fourier transform are both required. Another disadvantage is that the calibration error is very large due to limited sample snapshots [8]. For time-domain calibration method, filter coefficients are calculated by adaptive filtering algorithm in iteration. So the implement is much simple. Chirp signal is proposed as the reference signal in [9]. However, the weight vector of adaptive equalizer cannot converge because chirp signal is a non-stationary signal. The proposed algorithm chooses the Binary Phase Shift Keying (BPSK) signal as the reference signal. Computer simulation results show that this method can achieve stable weight vector and well calibration performance.

The remaining paper is organized as follows. Section 2 describes the principle of calibration. Section 3 demonstrates the signal model and proposed methodology for the new time-domain calibration. The performance analysis is also illustrated in this section. The simulation results of the calibration with time-domain equalizer are given in Section 4. Finally Section 5 offers some conclusions.

2. **Principle of Channel Calibration.** Supposing the broadband receiving array antenna consists of $M + 1$ elements, channel 0 is the reference and the other channels are considered with mismatch. The block diagram of array antenna is shown as Figure 1 where reference channel and only one calibrated channel are illustrated for the sake of simplicity. Because of the mismatch, the channel transfer function $C_m(\omega)$ of the mth mismatch channel is not equal to the transfer function $C_{ref}(\omega)$ of the reference channel. So a transversal filter is employed between the front-end and digital beamformer to play the role of calibration.
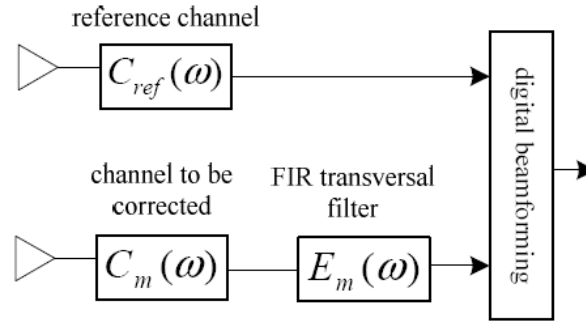
FIGURE 1. Principle diagram of array antenna

Then the overall transfer function of the mth channel is given by

$$H_m(\omega) = C_m(\omega) E_m(\omega) \quad 1 \le m \le M \tag{1}$$

Perfect calibration means that each $H_m(\omega)$ should be equal to $C_{ref}(\omega)$, namely

$$H_1(\omega) = H_2(\omega) = \cdots = H_M(\omega) = C_{ref}(\omega) \tag{2}$$

In that way, frequency response of the desired transversal filter must satisfy

$$E_m(\omega) = C_{ref}(\omega)/C_m(\omega) \tag{3}$$

3. **Filter Coefficients Calculation.**

3.1. **System structure and signal model.** To compute the coefficient $\boldsymbol{c}_m$ of the mth transversal filter, an equalizer with weight vector $\boldsymbol{w}_m$ is utilized which is connected as illustrated in Figure 2. In fact, the transversal filter and equalizer have the same structure with L order taps, so $\boldsymbol{c}_m$ and $\boldsymbol{w}_m$ are both $L + 1$ dimensional column vector. As Figure 2 shows, each equalizer works independently to obtain the weight vector $\boldsymbol{w}_m$.

The array is installed in microwave darkroom, where a BPSK signal $s(t)$ is transmitted from far field [10] and travels vertically on the surface of array. Of course, the spectrum of BPSK signal should cover operating band of the array antenna. Then the digital signal received by reference channel is described as $d(k)$. Similarly the input signal for the mth equalizers is $x_m(k)$. An adaptive filtering algorithm in time domain is deployed to compute $\boldsymbol{w}_m$ through k times iterations and converge to $\boldsymbol{w}_m = \boldsymbol{w}_m(k)$. Then the equalizer transfers the weight vector $\boldsymbol{w}_m$ to the transversal filter as coefficient $\boldsymbol{c}_m$, namely

$$\boldsymbol{c}_m = \boldsymbol{w}_m \tag{4}$$

3.2. **Weight vector calculation.** To calculate weight vector, the equalizer exploits Least Mean Squares (LMS) or Recursive Least Squares (RLS) adaptive filtering algorithm in time domain. Although RLS algorithm has a fast rate of convergence, the computational burden is much larger than LMS [11]. By contrast, the steady-state error for LMS algorithm can be adjusted to an acceptable level through the step size parameter [12].
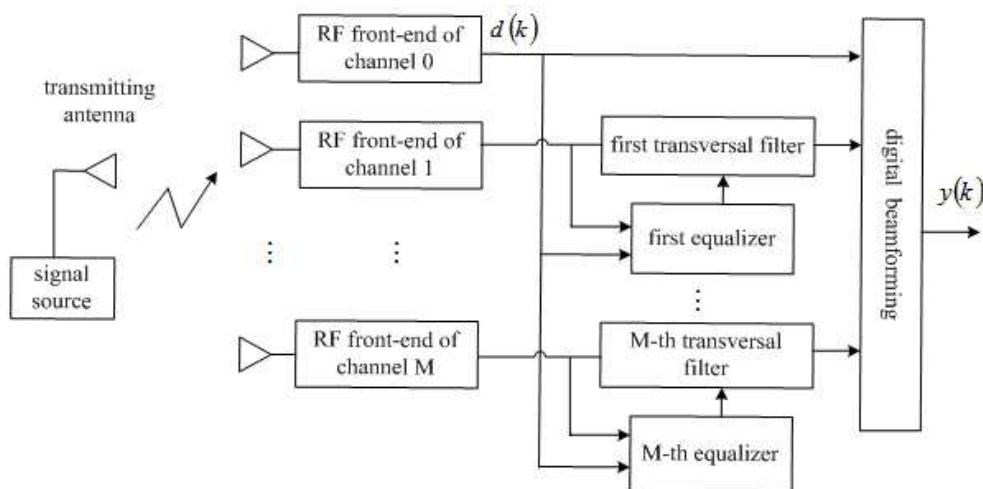
FIGURE 2. Diagram of time domain calibration method

The mth equalizer inputs include reference signal $d(k)$ and vector $\boldsymbol{x}_m(k)$, which consists of $L + 1$ continuous sample snapshots of $x_m(k)$ and is given by

$$\boldsymbol{x}_m(k) = [x_m(k) \quad \cdots \quad x_m(k-L)]^T \tag{5}$$

If $k < 0$, we set $x_m(k) = 0$. The mth equalizer uses LMS algorithm as following steps to get $\boldsymbol{w}_m$:

Step 1: when $k = 0$, select step-size μ and set $\boldsymbol{w}_m(0) = [0 \quad \cdots \quad 0]^T$;

Step 2: calculate the output error by

$$e_m(k) = d(k) - \boldsymbol{w}_m^H(k)\boldsymbol{x}_m(k) \tag{6}$$

where the operator "$[\ ]^H$" represents conjugate transpose;

Step 3: update the weight vector with

$$\boldsymbol{w}_m(k+1) = \boldsymbol{w}_m(k) + \mu e_m^*(k)\boldsymbol{x}_m(k) \tag{7}$$

where the operator "$*$" means conjugate;

Step 4: judge whether the weight vector has converged or not. If not, then set $k = k+1$ and jump to Step 2. Otherwise, the weight vector $\boldsymbol{w}_m(k)$ is served as the output weight vector $\boldsymbol{w}_m$ of equalizer and the iterative calculations are stopped.

Step 5: convey $\boldsymbol{w}_m$ to the transversal filter as the coefficient vector $\boldsymbol{c}_m$.

3.3. **Performance of the calibration.** Performance of the above method mainly includes convergence time and steady error. To insure the convergence [13], the range of step size is

$$0 < \mu < [LP_{in}]^{-1} \tag{8}$$

where P_{in} is the input signal power. The larger step size will cause faster convergence speed and worse steady state error.

In addition, the noise in the reference signal will degrade the accuracy of the weight vector, which does not happen in the classic LMS adaptive filter where the reference signal is noiseless. For the proposed algorithm, the reference signal is

$$d(k) = s(k) + n(k) \tag{9}$$

and the noise $n(k)$ will derive an additional error term in the solution for Winner-Hopf equation as [14]

$$\boldsymbol{w} = \boldsymbol{R}^{-1}\boldsymbol{p} = \boldsymbol{R}^{-1}\boldsymbol{p}_0 + \boldsymbol{R}^{-1}\boldsymbol{p}_n \tag{10}$$

In the above expression, the second term on the right side is external error resulting from noise where the covariance matrix $\boldsymbol{R}$ is defined as

$$\boldsymbol{R} = E\left[\boldsymbol{x}\left(k\right)\boldsymbol{x}^{H}\left(k\right)\right] \tag{11}$$

In addition, the cross-correlation vector between $\boldsymbol{x}(k)$ and $d(k)$ is

$$\boldsymbol{p} = E\left[\boldsymbol{x}\left(k\right)d^{*}\left(k\right)\right] = E\left[\boldsymbol{x}\left(k\right)s\left(k\right)\right] + E\left[\boldsymbol{x}\left(k\right)n\left(k\right)\right] = \boldsymbol{p}_{0} + \boldsymbol{p}_{n} \tag{12}$$

It is easy to prove that the error term $\boldsymbol{R}^{-1}\boldsymbol{p}_{n}$ could be reduced effectively by increasing the Signal to Noise Ratio (SNR) of reference signal [15].

4. **Simulation and Analysis.** Computer simulations are exploited to investigate the performance of new calibration methodology. Assuming the frequency response of reference channel $C_{ref}(\omega)$ is 1, the reference signal is a broadband BPSK signal with intermediate frequency of 50MHz and bandwidth of 20MHz. The tap number L of transversal filter and equalizer is 50 and the SNR is 50dB. The transmitted BPSK signal is received by reference channel and all mismatch channels respectively with the same SNR. The step size $\mu = 0.005$ can guarantee convergence. When the signal is normally incident upon the array, its phase offset between channels is generated only by the mismatch. Without loss of generality, simulation investigates only one channel with mismatch.

Figure 3 shows three amplitude frequency response curves. The channel function $C_{m}(\omega)$ utilizes sinusoid model and it is a convex plot in the figure. The bottom concave dash line is the amplitude spectrum $E_{m}(\omega)$ for the transversal filter whose coefficients come from the equalizer. The overall response is equal to

$$H_{m}\left(\omega\right) = E_{m}\left(\omega\right)C_{m}\left(\omega\right) \approx 1 = C_{ref}\left(\omega\right) \tag{13}$$

That proves the proposed methodology works well since Equation (2) is satisfied.
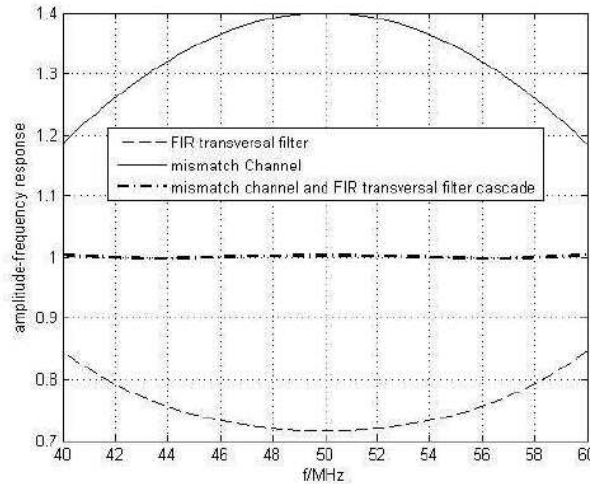
FIGURE 3. Amplitude frequency response curve in the pass band region

Figure 4 illustrates three signals in time domain, which are the BPSK reference, input and output waves of transversal filter. Obviously, the post-calibration signal coincides with the reference. That also proves the validity of proposed calibration strategy.

The step size of LMS algorithm deeply impacts the performance of calibration as shown in Figure 5. The residual error is defined as

$$\Delta H_{m}\left(\omega\right) = E_{m}\left(\omega\right)C_{m}\left(\omega\right) - 1 \tag{14}$$

Assuming the step size μ is 0.005, 0.01 and 0.018 respectively, the plots show that the best performance is achieved with the minimum step size. This result could be explained through the misadjustment analysis in LMS filtering theory.
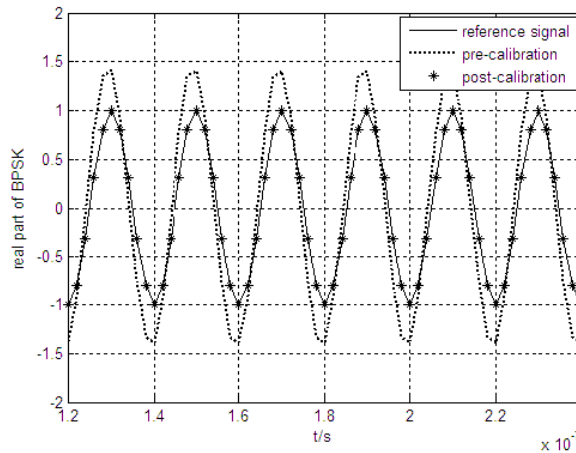
FIGURE 4. The BPSK signals with calibration
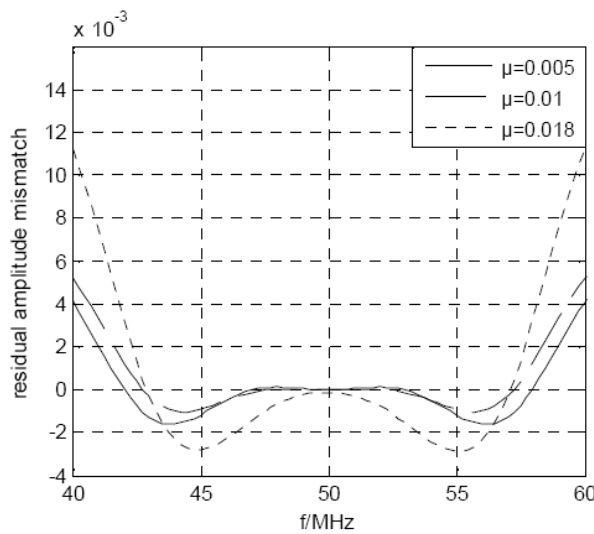
FIGURE 5. Residual amplitude mismatch with different step sizes

As discussed in the previous chapter, the SNR also plays an important role in the new approach due to the noisy reference signal. In Figure 6, we set SNR to be 20dB, 30dB and 50dB respectively and the residual errors are plotted. Obviously, the higher the SNR is, the less the error we obtain.

Finally, we study the relationship between the order of the transversal filter and calibration performance. As Figure 7 illustrated, the order L is set to 30, 40 and 50 respectively. Through the results, we can see that the larger tap number could generate less residual error especially in the region of pass band edge. However, the high order of filter will cause large group delay and more expenditure for hardware resource.

5. **Conclusions.** A time domain calibration method in broadband receiving array antenna is proposed in detail. Some simulation experiments prove its validity. Compared with frequency-domain calibration method, the proposed approach is much easier to implement from the engineering point of view due to low computational complexity. However, this strategy is limited by the microwave darkroom requirement. So we should explore a methodology to finish the calibration even when the array is installed on some platform, which is the future work.
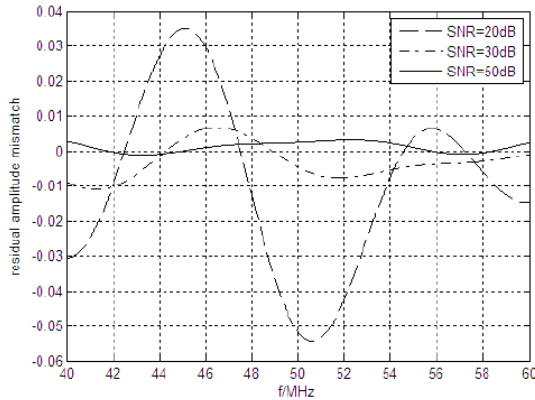
FIGURE 6. Residual amplitude mismatch with different SNR
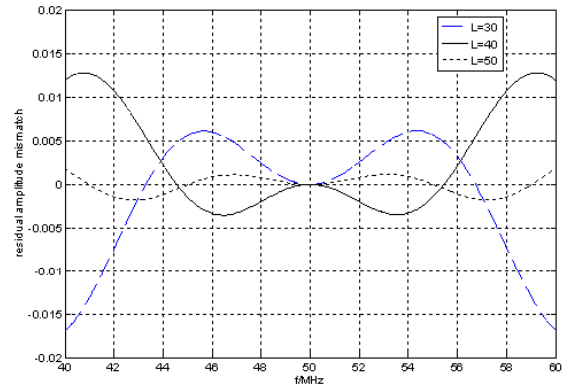
FIGURE 7. Residual amplitude mismatch with different tap numbers

REFERENCES

[1] D. C. Chang and C. N. Hu, Smart antennas for advanced communication systems, *Proc. of the IEEE*, vol.100, no.7, pp.2233-2249, 2012.

[2] X. R. Wang, E. Aboutanios and M. G. Amin, Reconfigurable adaptive array beamforming by antenna selection, *IEEE Trans. Signal Processing*, vol.62, no.9, pp.2385-2396, 2014.

[3] I. Moazzen and P. Agothoklis, Efficient implementation of broadband beamformers using nested hexagonal arrays and frustum filters, *IEEE Trans. Signal Processing*, vol.61, no.19, pp.4796-4805, 2013.

[4] D. T. Nguyen, R. Boyer and S. Marcos, On the angular resolution Limit for array processing in the presence of modeling errors, *IEEE Trans. Signal Processing*, vol.61, no.19, pp.4701-4706, 2013.

[5] M. S. Hossain, G. N. Milford and M. C. Reed, Efficient robust broadband antenna array processor in the presence of look direction errors, *IEEE Trans. Antennas and Propagation*, vol.61, no.2, pp.718-727, 2013.

[6] A. Broquetas, F. Lopez-Dekker and J. Closa, Evaluation of the internal calibration methodologies for space borne synthetic aperture radars with active phased array antennas, *IEEE Journal of Selected Topics in Applied Earth Observations and Remote Sensing*, vol.5, no.3, pp.909-918, 2012.

[7] A. Young, M. V. Ivashina and R. Maaskant, Improving the calibration efficiency of an arrayfed reflector antenna through constrained beamforming, *IEEE Trans. Antennas and Propagation*, vol.61, no.7, pp.3538-3545, 2013.

[8] L. C. Godara and M. R. S. Jahromi, Limitations and capabilities of frequency domain broadband constrained beamforming schemes, *IEEE Trans. Signal Processing*, vol.47, no.9, pp.2386-2395, 1999.

[9] C. Y. Feng and Y. M. Wu, The research of channel adaptive calibration of LFM signal based on NLMS, *Journal of Electronics & Information Technology*, vol.28, no.12, pp.2248-2251, 2006.

[10] T. Takahashi, Y. Konish and S. Makino, Fast measurement technique for phased array calibration, *IEEE Trans. Antennas and Propagation*, vol.56, no.7, pp.1888-1899, 2008.

[11] B. C. Banister and J. R. Zejdler, Tracking performance of the RLS algorithm applied to an antenna array in a realistic fading environment, *IEEE Trans. Signal Processing*, vol.50, no.5, pp.1037-1050, 2002.

[12] P. C. Wei, J. Han and J. R. Zeidler, Comparative tracking performance of the LMS and RLS algorithms for chirped narrowband signal recovery, *IEEE Trans. Signal Processing*, vol.50, no.7, pp.1602-1609, 2002.

[13] H. S. Lee, S. E. Kim and J. W. Lee, A variable step-size diffusion LMS algorithm for distributed estimation, *IEEE Trans. Signal Processing*, vol.63, no.79, pp.1808-1820, 2015.

[14] S. Haykin, *Adaptive Filter Theory*, 5th Edition, Prentice Hall, 2013.

[15] W. K. Kahn, Degradation in performance of adaptive null-steering antennas, *IEEE Trans. Antennas and Propagation*, vol.35, no.12, pp.1469-1473, 1987.